

DETECTION OF CONTACT BINARIES USING SPARSE HIGH PHASE ANGLE LIGHT CURVES

PEDRO LACERDA

Institute for Astronomy, University of Hawaii, 2680 Woodlawn Drive, Honolulu, HI 96822; pedro@ifa.hawaii.edu

Received 2007 July 25; accepted 2007 November 14; published 2007 December 3

ABSTRACT

We show that candidate contact binary asteroids can be efficiently identified from sparsely sampled photometry taken at phase angles $\alpha > 60^\circ$. At high phase angle, close/contact binary systems produce distinctive light curves that spend most of the time at maximum or minimum (typically >1 mag apart) brightness with relatively fast transitions between the two. This means that a few (approximately five) sparse observations will suffice to measure the large range of variation and to identify candidate contact binary systems. This finding can be used in the context of all-sky surveys to constrain the fraction of contact binary near-Earth objects. High phase angle light-curve data can also reveal the absolute sense of the spin.

Subject headings: minor planets, asteroids — solar system: general — techniques: photometric

1. INTRODUCTION

For most purposes, small solar system bodies are best observed at solar opposition. Measurements taken at low phase angle (the Sun-target-observer angle, denoted α ; see Fig. 1) benefit from strong backscattering, thus rendering the target brighter. In astrometric or surface-averaged measurements, the enhanced signal-to-noise ratio due to the low phase angle geometry is desirable. However, if the goal is to derive information on the shape of the target, then high- α data become useful. This has been noted in the past, in the context of light-curve inversion problems (Ďurech & Kaasalainen 2003). As a body rotates, the amount of sunlight it reflects to the observer depends on the time-varying-projected cross section, which in turn depends on its shape. If well-sampled light-curve information is obtained at multiple observing geometries, then the shape of the object can be derived. At low phase angles, the nonconvex features of an object are not apparent from its light curve. This means that, in the absence of high- α data, the nonconvex figure of a contact binary can be wrongly interpreted as being composed of a single convex component.

One known effect of high- α observations on light curves is the increase in the peak-to-peak range of variation (Gehrels 1956). For single ellipsoidal bodies, and for phase angles $\alpha < 40^\circ$, the light-curve range Δm has been shown to vary roughly linearly with α (Zappala et al. 1990). This is generally known as the amplitude-phase relationship (APR). When observing from Earth, the maximum phase angle at which a small solar system body can be imaged depends essentially on its heliocentric distance. The distant Kuiper Belt objects can be observed at up to $\alpha \sim 2^\circ$, Jovian Trojan asteroids at $\alpha \lesssim 10^\circ$, and main-belt asteroids at $\alpha \lesssim 30^\circ$. Only near-Earth objects (NEOs) can be observed at phase angles $\alpha > 30^\circ$, which makes them the best candidates for high- α studies.

On the order of 20 binary NEOs have been discovered, both photometrically (e.g., Pravec & Hahn 1997; Pravec et al. 1998) and from radar observations (e.g., Nolan et al. 2000; Ostro et al. 2002). From the known sample, it is possible to note a few characteristic features (Pravec et al. 2006). The primaries have mean diameters of ~ 1 km (with a spread of 1 order of magnitude), usually 2–4 times those of their secondary companions. One case, 69230 Hermes, has a size ratio close to unity (Margot et al. 2003). The separation distances are small, usually a few primary radii, and the mutual orbits are nearly circular. Most measured primaries spin (around the shortest physical axis)

close to the critical breakup rate for strengthless bodies with mean density ~ 2 g cm $^{-3}$. The secondaries have synchronized spin and orbital periods. In the few (~ 10) cases in which shapes can be inferred, the primaries are well described by oblate spheroids, whereas the secondaries have elongated shapes along the line of centers. One NEO, 4769 Castalia, is suspected from radar data to be a contact binary (Ostro et al. 1990).

In recent years, explanations as to how binary NEOs may form have mostly converged on the idea of the splitting of a parent body. Weidenschilling (1980) proposed that binaries may form by rotational fission of an object affected by an off-center impact. Margot et al. (2002) argued that spin-up due to tidal interactions during close encounters with planets was the most likely formation process for NEO binaries, and Bottke et al. (2006) were the first to suggest that radiation forces (the Yarkovsky-O'Keefe-Radzievskii-Paddack [YORP] effect) provide the torque needed for rotational fission. The main features of the NEO binary sample described above have led Ćuk (2007) to propose the following formation mechanism: due to the YORP effect, ~ 1 km objects are spun up close to breakup rates, which leads to the accumulation of regolith around the equator. As the YORP effect continues to spin up the body, the surface material is eventually stored in orbit around the (now) primary, where it coagulates into a secondary; the latter grows into an elongated, nearly Roche-equilibrium shape that balances gravitational and inertial accelerations. The subsequent evolution of the mutual orbit is driven by the BYORP effect, the binary version of the YORP effect, which may lead the components away from each other but may also bring them together in mutual contact (Ćuk & Burns 2005; Scheeres 2007).

Obtaining a well-sampled light curve of an NEO that is capable of unequivocally establishing its nature would require extensive observations at multiple geometries. For a sparse survey, such as will be undertaken by the Panoramic Survey Telescope and Rapid Response System (Pan-STARRS; typically revisiting each target ~ 4 times per lunation), it may take years before the shape of the object can be determined. The method presented here can single out potential contact binaries after approximately five measurements at high α . In this Letter, we present the first light-curve simulations of contact binaries at high phase angle, and we use them to address the detectability of such systems.

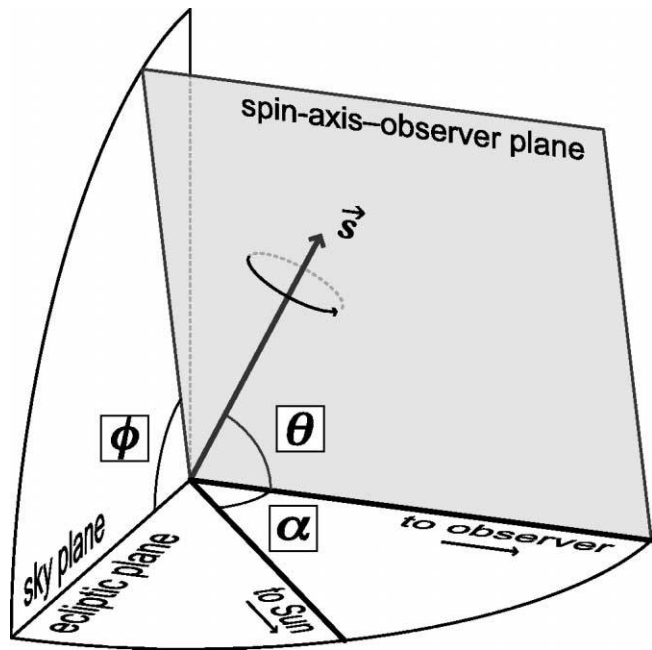


FIG. 1.—Angles used to describe the observing geometry. The orbital spin axis is denoted s . The contact binary is assumed to be located at the vertex where the angles θ (aspect, the angle between the orbital spin axis and the line of sight), α (phase, the angular distance between the Sun and the observer, as seen from the object), and ϕ (azimuth, the sky-plane angle between the projections of the orbital spin axis and the object-Sun vector) are measured.

2. HIGH PHASE ANGLE LIGHT CURVES

The characteristic morphological features of contact binary light curves are the large range of variation, typically 0.9 mag or more, the rounded, inverted-U-shaped maxima, and the sharp V-shaped minima (Zappala et al. 1980; Leone et al. 1984).

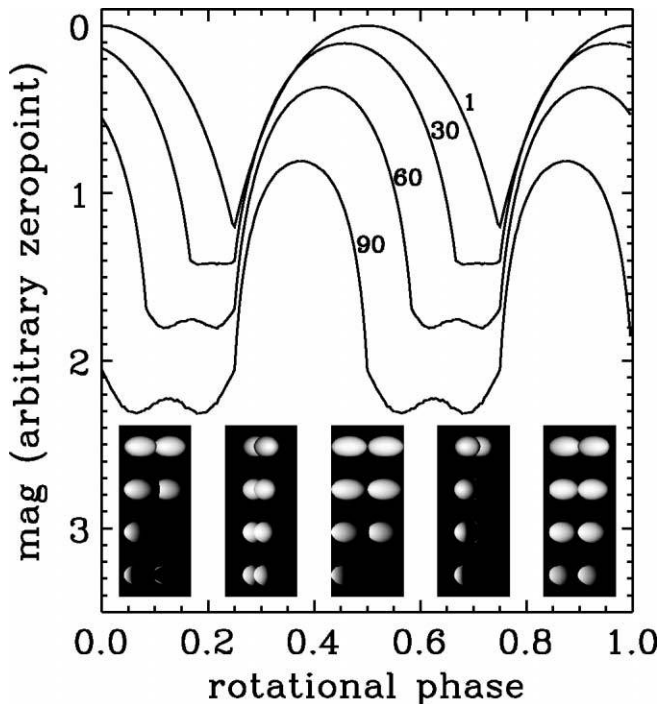


FIG. 2.—Change in light-curve morphology with increasing phase angle. Lines are labeled with the corresponding phase angles ($\alpha = 1^\circ, 30^\circ, 60^\circ,$ and 90°). Insets show rendering of the binary used to produce the light curves (phase angle increasing from top to bottom) at rotational phases $\phi = 0.1^\circ, 0.3^\circ, 0.5^\circ, 0.7^\circ,$ and 0.9° .

TABLE 1

FOUR CLOSE/CONTACT BINARY SYSTEMS CONSIDERED

System	q^a	(B/A, C/A) ^b	(b/a, c/a) ^c	l^d	H.E. ^e
1	1.00	(0.66, 0.60)	(0.66, 0.60)	1.00	Yes
2	0.67	(0.77, 0.69)	(0.53, 0.49)	1.00	Yes
3	0.25	(0.92, 0.83)	(0.51, 0.48)	1.19	Yes
4	0.13	(1.00, 0.90)	(0.51, 0.48)	1.00	No

^a Mass ratio.
^b Primary axis ratios.
^c Secondary axis ratios.
^d Orbital distance in units of $A + a$.
^e Components in hydrostatic equilibrium.

However, these traits appear only at phase angles close to $\alpha = 0^\circ$. Figure 2 shows light curves of a symmetric contact Roche binary (system 1 from Table 1) at four different phase angles, $\alpha = 1^\circ, 30^\circ, 60^\circ,$ and 90° . The surface scattering of light is modeled using a Lommel-Seeliger function, taken to represent a low-albedo, lunar-type surface. The procedure used for generating the model light curves of Roche binaries, as well as of Jacobi triaxial ellipsoids, is described in detail in Lacerda & Jewitt (2007). As α increases, the most noticeable mutations are as follows:

1. The shape of the minimum changes from a V shape to a flat shape to a slightly W shape.
2. The transition between low and high brightness becomes sharper.
3. The positions (in rotational phase) of the minima and maxima drift to the left.
4. The overall brightness decreases, as the illuminated fraction of the surface diminishes.
5. The trough-to-peak range of variation increases.

Below, we discuss some of these points in more detail.

2.1. Light-Curve Shape and Detection Probability

As a consequence of points 1 and 2 above, the probability of detecting the total range of brightness variation from only a few measurements increases significantly with α . This is shown in Figure 3, where we plot the probability of measuring the extent of variation of a contact binary light curve for different values of α . Figure 3 was generated as follows: each of the four light curves in Figure 2 (corresponding to each α) was sampled five times at random rotational phases, and the maximum range Δm_i within the set of five measurements was reg-

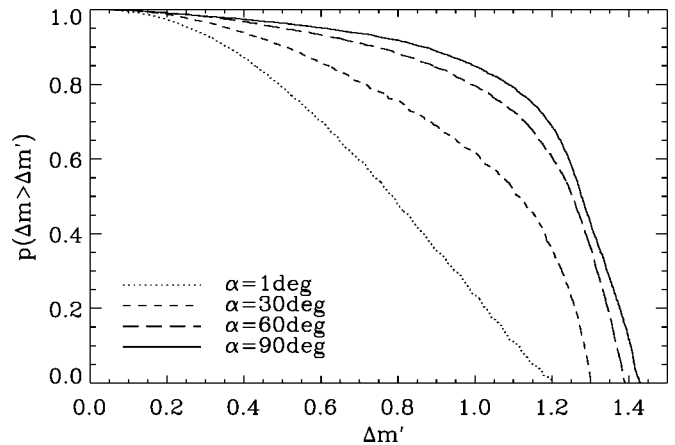


FIG. 3.—Probability of measuring a magnitude range larger than $\Delta m'$ from random sampling each light curve in Fig. 2 five times. An observing geometry $\theta = \phi = 90^\circ$ has been assumed (see text and Fig. 1).

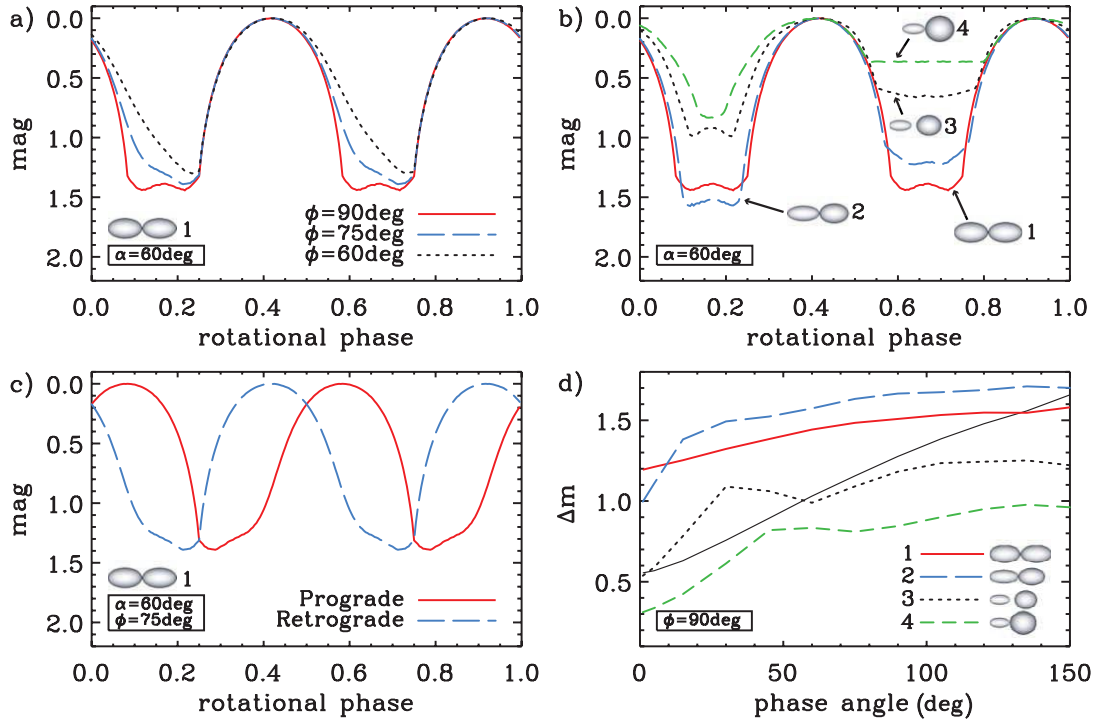


FIG. 4.—(a) Light curves of system 1 (Table 1) as a function of azimuth angle ϕ . The geometry is $\alpha = 60^\circ$. (b) Light curves of all four systems in Table 1 at $\alpha = 60^\circ$ and $\phi = 90^\circ$. (c) Asymmetric light curves of system 1 rotating in the prograde and retrograde directions. The asymmetry is due to an observing geometry $\phi \neq 90^\circ$ and a high phase angle $\alpha = 60^\circ$ and shows clear dependence on the direction of rotation of the binary. (d) Light-curve range vs. phase angle ($\alpha = 1^\circ, 5^\circ, 15^\circ, 30^\circ, 45^\circ, 60^\circ, 75^\circ, 90^\circ, 105^\circ, 120^\circ, 135^\circ, \text{ and } 150^\circ$) for each system in Table 1. The thin solid black line corresponds to a Jacobi ellipsoid with axes ratios $b/a = 0.60$ and $c/a = 0.43$. The observing geometry is $\phi = 90^\circ$ (Fig. 1). All four plots assume Lommel-Seeliger lunar-type surface scattering and aspect angle $\theta = 90^\circ$.

istered. This procedure was then repeated for $i = 1-10,000$, and the cumulative distribution of ranges Δm_i was plotted for each α , starting from the maximum range. The plot shows that, beyond $\alpha \sim 60^\circ$, most five-point samples of the light curve are able to identify a variation larger than 1 mag. For example, at $\alpha = 60^\circ$, there is an $\sim 80\%$ chance of detecting a $\Delta m \geq 1$ mag from five sparse observations of the contact binary considered.

Figure 3 was obtained by assuming the most favorable observing geometry (Fig. 1): $\theta = 90^\circ$, measured between the spin pole and the line of sight, and $\phi = 90^\circ$, measured in the plane of the sky between the spin pole and the object-Sun vector. The total range of a contact binary light curve decreases with the aspect angle θ at about $0.03-0.04 \text{ mag deg}^{-1}$ (Lacerda & Jewitt 2007); the maximum range is obtained at $\theta = 90^\circ$. The azimuthal angle ϕ also influences the light-curve range and shape. As ϕ moves away from 90° (the direction does not matter), the light curve becomes asymmetric and the range of variation is slightly decreased (Fig. 4a). Therefore, requiring a favorable geometry (i.e., angles larger than chosen minimum values $\theta > \theta_m$ and $\phi > \phi_m$) reduces the probability of detection of large Δm . Assuming randomly oriented spin axes, the probability of having simultaneously favorable θ and ϕ is given by

$$1 - \frac{2}{4\pi} \left[\int_0^{\theta_m} \int_0^{2\pi} \sin(\theta) d\phi d\theta + \int_{\theta_m}^{\pi/2} \int_{-\phi_m}^{\phi_m} \sin(\theta) d\phi d\theta \right] \\ = \frac{(\pi - \phi_m)}{\pi} \cos(\theta_m),$$

which, for minimum aspect and azimuth $\theta_m = \phi_m = 75^\circ$, is ~ 0.15 . This probability must be taken into account when estimating the intrinsic fraction of contact binary systems from

a sparsely sampled survey. At any rate, since the geometry constraint (dominated by θ) is present at all phase angles, the conclusion that high- α measurements are more effective at identifying contact binary systems holds.

Figure 4b shows how the light-curve shape depends on the relative size and separation of the binary components. Four systems were considered; their properties are detailed in Table 1. Except for system 3, which is meant to represent a system formed according to the model by Āuk (2007) mentioned in § 1, all systems are Roche binaries in hydrostatic equilibrium. Systems 3 and 4 produce shallower light curves due to their asymmetric mass ratio, and although the maxima and minima take up a large fraction of the rotational phase, the probability of measuring the total range of variation is not as high as for the more symmetric binary systems 1 and 2. In conclusion, high- α observations will more easily detect contact binaries with similar sized components.

Currently known binary NEOs are generally asymmetric, with primary to secondary size ratios of 2–4 (Pravec et al. 2006). Furthermore, no very close pairs or contact binaries have been directly observed (with the possible exception of 25143 Itokawa; Scheeres et al. 2007). The minimum orbital period is $P = 11$ hr. Whether these are intrinsic features or the result of observational bias is still unclear, but the aptness of the method presented here to find symmetric contact binaries should help throw light on the subject. The intrinsic fraction of close and contact binaries is a powerful constraint for models of NEO binary formation and destruction.

2.2. Light-Curve Phase Shift and Spin Direction

Increasing the phase angle α produces a shift in the rotational phase of the light curves (see Fig. 2). The shift happens, respectively, to the left or right, depending on the object being

illuminated from the left or right side, from the observer's standpoint. We measure a linear rotational phase shift with a slope $\sim 1.4 \times 10^{-3} \text{ deg}^{-1}$ phase angle. The shift slope is similar for all four systems in Table 1. This effect must be taken into account when fitting a single rotation period to data taken at different phase angles, if not to be confused with evidence for complex rotation.

As mentioned in § 2.1, if the geometry is such that $\phi \neq 90^\circ$, then asymmetries arise in the light curve. The direction of the asymmetry depends on the sense of rotation of the binary. Figure 4c illustrates this effect. The asymmetry can thus be used to infer the sense of spin of the binary.

2.3. Light-Curve Range

Careful inspection of Figure 2 shows that the light-curve range increases with α . This is more easily seen in Figure 4d, where the light-curve range is plotted versus phase angle (APR) for each of the four systems in Table 1. For comparison, a thin black solid line illustrates the same dependence for a triaxial Jacobi ellipsoid with axis ratios $b/a = 0.60$ and $c/a = 0.43$.

We find that, with the exception of the symmetric binary system 1, the APRs of binary systems appear less regular than that of the ellipsoid. Binary APRs show two roughly linear regimes, steeper for lower α and shallower for larger α . The slope only seems to depend on system type for small to intermediate phase angles: beyond $\alpha \sim 50^\circ$, the slopes are similar for all systems. Systems with smaller ranges at $\alpha = 1^\circ$ have shallower initial APR slopes. This is similar to what was found by Zappala et al. (1990) for ellipsoids. System 1, however, has a remarkably regular APR. The slope is $0.004 \text{ mag deg}^{-1}$ up to $\alpha \sim 75^\circ$ and $0.001 \text{ mag deg}^{-1}$ beyond that value. Incidentally, the symmetric binary 90 Antiope (Merline et al. 2000; Descamps et al. 2007) has an APR slope $0.005 \text{ mag deg}^{-1}$ (Michałowski et al. 2002), very close to that of our simulated symmetric binary. The APR is shape-dominated: the APR slopes do not depend significantly on the choice of surface scattering model.

Our results seem to indicate that less regular (more asym-

metric) objects have steeper APRs. Our most regular object, the symmetric binary, has the shallowest APR. A detailed analysis of the APR of contact binary systems is beyond the scope of this Letter and will be treated elsewhere.

3. SUMMARY

We have presented the case for using high phase angle observations to find extreme light curves produced by contact binaries in the solar system. Sparse observations of contact binaries at phase angles $\alpha > 60^\circ$ are extremely efficient at detecting the large range of brightness variation characteristic of these objects' light curves. From Earth, this method is most relevant to observations of near-Earth objects as they attain the largest phase angles. At this point, a survey of high- α measurements alone should probably not be used to estimate the fraction of contact binaries in the NEO population. Deviations from hydrostatic equilibrium shape and the precise observing geometry (θ and ϕ) affect the exact detection probability, thereby introducing uncertainty in the derived abundance. The technique is extremely efficient at detecting equator-on, relatively smooth contact binaries with symmetric components, but confirmation of the exact configuration of a system that shows large Δm in just a few high- α measurements should always be sought using follow-up observations. The sparse quality of planned all-sky surveys such as Pan-STARRS implies that a full shape solution can be obtained only after several years of data have been collected. It is therefore extremely useful to develop fast techniques that allow the identification of potentially interesting targets from a Pan-STARRS-type survey (or even from dedicated surveys using sub-1 m telescopes), which can be followed up on other telescopes.

I thank David Jewitt for insightful discussions and comments on the manuscript, and for correctly predicting that I was going to write it. I also acknowledge Nuno Peixinho for helpful comments. This work was supported by a grant from NSF to David Jewitt.

REFERENCES

- Botke, W. F., Jr., Vokrouhlický, D., Rubincam, D. P., & Nesvorný, D. 2006, *Annu. Rev. Earth Planet. Sci.*, 34, 157
- Čuk, M. 2007, *ApJ*, 659, L57
- Čuk, M., & Burns, J. A. 2005, *Icarus*, 176, 418
- Descamps, P., et al. 2007, *Icarus*, 187, 482
- Đurech, J., & Kaasalainen, M. 2003, *A&A*, 404, 709
- Gehrels, T. 1956, *ApJ*, 123, 331
- Lacerda, P., & Jewitt, D. C. 2007, *AJ*, 133, 1393
- Leone, G., Paolicchi, P., Farinella, P., & Zappala, V. 1984, *A&A*, 140, 265
- Margot, J. L., Nolan, M. C., Benner, L. A. M., Ostro, S. J., Jurgens, R. F., Giorgini, J. D., Slade, M. A., & Campbell, D. B. 2002, *Science*, 296, 1445
- Margot, J. L., et al. 2003, *IAU Circ.*, 8227, 2
- Merline, W. J., Close, L. M., Dumas, C., Shelton, J. C., Menard, F., Chapman, C. R., & Slater, D. C. 2000, *BAAS*, 32, 1017
- Michałowski, T., Colas, F., Kwiatkowski, T., Kryszczyńska, A., Velichko, F. P., & Fauvaud, S. 2002, *A&A*, 396, 293
- Nolan, M. C., Margot, J.-L., Howell, E. S., Benner, L. A. M., Ostro, S. J., Jurgens, R. F., Giorgini, J. D., & Campbell, D. B. 2000, *IAU Circ.*, 7518, 2
- Ostro, S. J., Chandler, J. F., Hine, A. A., Rosema, K. D., Shapiro, I. I., & Yeomans, D. K. 1990, *Science*, 248, 1523
- Ostro, S. J., Hudson, R. S., Benner, L. A. M., Giorgini, J. D., Magri, C., Margot, J. L., & Nolan, M. C. 2002, in *Asteroids III*, ed. W. F. Bottke Jr., et al. (Tucson: Univ. Arizona Press), 151
- Pravec, P., & Hahn, G. 1997, *Icarus*, 127, 431
- Pravec, P., Wolf, M., & Sarounova, L. 1998, *Icarus*, 133, 79
- Pravec, P., et al. 2006, *Icarus*, 181, 63
- Scheeres, D. J. 2007, *Icarus*, 189, 370
- Scheeres, D. J., Abe, M., Yoshikawa, M., Nakamura, R., Gaskell, R. W., & Abell, P. A. 2007, *Icarus*, 188, 425
- Weidenschilling, S. J. 1980, *Icarus*, 44, 807
- Zappala, V., Cellino, A., Barucci, A. M., Fulchignoni, M., & Lupishko, D. F. 1990, *A&A*, 231, 548
- Zappala, V., Scaltriti, F., Farinella, P., & Paolicchi, P. 1980, *Moon Planets*, 22, 153